THE ASTROPHYSICAL JOURNAL, 403:211–215, 1993 January 20

CONTINUOUS ABSORPTION OF He I λ10830 IN PLANETARY NEBULAE

J. KINGDON AND G. J. FERLAND
Astronomy Department, The Ohio State University, Columbus, OH 43210
Received 1992 May 7; accepted 1992 July 22

ABSTRACT

Several recent studies have found that the observed intensity of He I λ10830 in planetary nebulae is roughly one-half of that predicted by theory. This implies that the mechanisms populating the $2\,^3S$ level of neutral helium are not yet understood. This discrepancy must be accounted for in order to assess the importance of collisional effects in He I and to accurately determine helium abundances. In this paper, we examine the extent to which internal dust in planetary nebulae can affect the emitted λ10830 intensity. We present approximate correction factors for the λ10830 intensity, and examine how the line ratio λλ10830/5876 and the IR excess vary as a function of the dust fraction and the electron density. We find that destruction by dust is very significant for nebulae which are optically thick in λ10830, and that the size of this effect is strongly dependent on the dust fraction. We also briefly discuss the serious observational uncertainties in the measurement of the λ10830 line. Given these observational uncertainties, and the uncertainties in the dust-to-gas ratio, we conclude that there is no strong evidence of an extra depopulation mechanism for the $2\,^3S$ level.

Subject headings: atomic processes — dust, extinction — planetary nebulae: general

1. INTRODUCTION

Helium abundances must be accurately known for studies of stellar evolution, galactic chemical evolution, and the primordial helium abundance. Abundance determinations are complicated by the metastable $2\,^3S$ level in He I. Ferland (1986) recently called attention to the importance of collisions from this level for the resultant line spectrum. Using the quantal calculations of Berrington et al. (1985), he found that ignoring these collisional effects would result in the He abundance in planetary nebulae (PNs) being overestimated by as much as 50%. More recent quantal calculations (Berrington & Kingston 1987) have reduced this number to a maximum of roughly 30% (Clegg 1987), but the importance of collisions in the He spectrum persists.

Inclusion of these collisional effects in He abundance calculations has been hampered by a long-standing discrepancy in the intensity of He I λ10830 ($2\,^3S$–$2\,^3P$). It has been suspected for several decades now (cf. Osterbrock 1964) that the observed intensity of this line, which is primarily collisionally excited, is substantially weaker than predicted by standard theory. Improvements in both theory and observation have narrowed this discrepancy to a factor of ~2. Based on this, Peimbert & Torres-Peimbert (1987) and Péquignot, Balateau, & Gruenwald (1988) postulated that the $2\,^3S$ level is being depopulated by some previously unconsidered mechanism. This in turn led them to conclude that collisional effects are negligible, except in type I PNs, where they would be very small. However, theoretical attempts to account for this unknown depopulation mechanism have proven unsuccessful (cf. Clegg & Harrington 1989), and future work along this line does not look promising.

A rather different approach is to assume that the predicted level population for $2\,^3S$ is correct, but that some other effect weakens the λ10830 intensity. Kingdon & Ferland (1991) showed that absorption by water vapor in Earth's atmosphere reduced the observed λ10830 intensity in the PN NGC 7027 by ~25%. An earlier idea, suggested independently by Persson (1970) and Robbins (1970), is that λ10830 is partially destroyed by dust grains within the nebula. The destruction effect of continuous opacity such as grains is significantly enhanced if a line is optically thick. Persson found that for reasonable dust parameters, this effect could completely explain the discrepancy. More recently, Le Van & Rudy (1983) found that the size of the discrepancy increased with the planetary's electron density and showed that a simple dust model could account for the observed correlation. However, the importance of dust in resolving this problem remains unsettled, although it is clear that dust effects must be considered since depletion patterns show that dust does exist in the ionized regions of PNs (cf. Kingdon & Ferland 1993).

In this paper, we again examine the effect of dust on the intensity of the λ10830 line. In § 2, we present a simplified formalism for determining the size of this effect and give results for a small sample of PNs. In § 3, we calculate the effect of dust and the electron density on the λλ10830/5876 line ratio and the IR excess by using a photoionization model. Finally, we discuss our results in § 4.

2. A CORRECTION FACTOR FOR THE λ10830 INTENSITY

2.1. *General Procedure*

In this section we present an approximate formalism to determine the effect of dust on λ10830. In the following subsection, we apply this formalism to a small sample of PNs and show that it agrees well with more extensive numerical calculations.

The level population balance for the $2\,^3P$ state of He I is given by

$$N_e(N_p\,\alpha_{2\,^3P} + N_{2\,^3S}\,q_{2\,^3S,2\,^3P}) = N_{2\,^3P}(N_e\,q_{2\,^3P,2\,^3S} + A_{2\,^3P,2\,^3S}\epsilon)\,, \qquad (1)$$

where $\alpha_{2\,^3P}$ is the recombination rate coefficient to $2\,^3P$, the q_{ij} are the collisional rate coefficients, and ϵ is the escape probability. We have followed the standard convention of ignoring direct stellar excitation in equation (1) (i.e., a term

$N_{2\,^3S}B(2\,^3S–2\,^3P)I_\nu$ on the left-hand side of the equation), since this effect is completely negligible in this case. Also, for the electron densities present in PNs, collisional de-excitation from $2\,^3P$ is very small compared to radiative de-excitation. Thus, we ignore the first term on the right-hand side of equation (1). (This is valid for $N_e \ll 10^{13}$.)

For a nebula in which dust is present, the escape probability in equation (1) is modified to contain an extra term (cf. Netzer, Elitzur, & Ferland 1985). This gives

$$\epsilon' = \epsilon + \delta\,, \tag{2}$$

where δ represents the destruction of the λ10830 photon by dust. We shall discuss the exact form of δ later on.

The emitted intensity of λ10830 is given by

$$j_{10830} = \left(\frac{h\nu_{10830}}{4\pi}\right) N_{2\,^3P} A_{2\,^3P,2\,^3S} \epsilon\,. \tag{3}$$

Substituting equation (1), modified as discussed above into equation (3), we obtain

$$j_{10830} = \left(\frac{h\nu_{10830}}{4\pi}\right) N_e (N_p \alpha_{2\,^3P} + N_{2\,^3S} q_{2\,^3S,2\,^3P}) \left(\frac{\epsilon}{\epsilon + \delta}\right). \tag{4}$$

Note that in the absence of dust, the last term in parentheses in equation (4) would be equal to unity. Thus, the effect of dust is to reduce the λ10830 line intensity by a factor of $\epsilon/(\epsilon + \delta)$. Therefore, it is this ratio, hereafter designated by f, that we need to calculate.

We define a normalized destruction probability which is given by

$$\delta = (1 - \epsilon)\beta F(\beta) \tag{5}$$

(cf. Hummer 1968), where β is simply the ratio for continuous to total (continuous plus line) opacity, i.e.,

$$\beta = \frac{k_C}{k_L + k_C}\,, \tag{6}$$

with k the absorption coefficient in cm^{-1}. $F(\beta)$ is a known, tabulated function of β (cf. Hummer 1968, Table 1). The continuous opacity due to embedded grains can be conveniently rewritten as $\sigma_C N_{\rm H}$, with σ_C the cross section for continuous opacity (Draine & Lee 1984) and $N_{\rm H}$ the total hydrogen density likewise, the line absorption coefficient for λ10830 is

$$k_L = N_{2\,^3S}\left(\frac{\pi^2 e^2 f_{10830}}{m_e c \Delta\nu_D}\right). \tag{7}$$

Note that this is the *normalized* or mean line absorption coefficient, following Hummer, rather than the line center value. The population of $N_{2\,^3S}$ is then determined by the results of Clegg (1987) to be

$$N_{2\,^3S} = \left(\frac{5.79 \times 10^{-6} t_e^{-1.18}}{1 + 3110 t_e^{-0.51} N_e^{-1}}\right) N_{\rm He^+}\,. \tag{8}$$

Thus, the factor f is seen to be a simple function of temperature, density, and optical depth.

2.2. *Calculations and Results*

Although the above formalism can easily be incorporated into a photoionization model, for this paper we shall develop a formalism which will allow us to determine f for a series of PNs for which the input parameters are known. We shall calculate a more rigorous model later in this section, in which depth effects are taken into account. This model will be shown to agree well with the simplified technique discussed here.

Our approximation consists of considering the entire λ10830-producing zone to be represented by a single point, defined by an average T and N_e, and located at one-half the total optical depth of λ10830. We have considered each member of the λ10830 triplet separately, with the relative intensities determined by the statistical weights. The escape probability $\epsilon(\tau)$ was calculated by the approximate formulae for the K_2 function presented by Hummer (1981). We have taken $\sigma_C = 1 \times 10^{-22}$ cm^2 for the general interstellar medium (ISM) from Draine & Lee (1984). Finally, we take $N_{\rm He^+} = N_{\rm He} = 0.1 N_{\rm H}$.

We have calculated f as described above for several PNs listed in Clegg & Harrington (1989). The pertinent information is given in Table 1 and is taken directly from the above source, with the exception of the Meudon model, which will be discussed shortly. Columns (1), (2), & (3) list the nebula's name, average electron temperature (in units of 10^4 K), and average electron density, respectively. Column (4) gives the total optical depth in λ10830. Note again that this is the *mean* optical depth and is related to the line center optical depth by $\tau_{\rm mean} = \sqrt{\pi}\,\tau_0$. The dust-to-gas ratio by mass as a fraction of the ISM dust-to-gas ratio is listed in column (5). This number multiplies the continuum cross section σ_C given for the ISM above. The values in column (5) were obtained by dividing the values R in Table 2 of Clegg & Harrington (1989) by 0.007 (cf. Savage & Mathis 1979). The results of the calculations are presented in column (6). We see that the effect of dust on λ10830 is only a few percent for IC 418, NCC 7662, and IC 3568, and IC 3568, using the listed parameters. However, the effect is appreciable for DDDM-1 and Vy2-2. The latter is an extremely dense, compact nebula.

We now wish to test the accuracy of our approximation. To this end, we have run a photoionization model for the Meudon PN. This object is a test case introduced at the Paris Work shop on Model Nebulae (1986) and is intended to roughly approximate the well-studied PN NGC 7027. We have utilized G. J. Ferland's "Cloudy" photoionization code (Ferland 1992). This code incorporates the formalism described in the previous subsection, but integrates the results over a self-consistent ionization and thermal structure. The pertinent input parameters are listed in Table 2. The temperature and optical depth listed in Table 1 for Meudon are the results of this model. We determined f by running Cloudy with an amount of grains equal to the ISM, and then again with the same parameters but with the destruction probability set to zero. We then simply took the ratio of the emitted λ10830 intensity for the two cases. A spherical geometry was assumed

TABLE 1

NEBULA PARAMETERS

Name (1)	N_e (2)	T_e (3)	τ(10830) (4)	Dust/Gas (5)	f (6)
IC 418	1.45 (4)	0.85	373.2	0.1886	0.93
NGC 7662	2.47 (3)	1.31	68.2	0.0871	0.98
IC 3568	2.63 (3)	1.16	58.2	0.3571	0.96
DDDM-1	6.61 (3)	1.21	480.8	0.2143	0.82
Vy2-2	3.21 (5)	1.03	2592.2	0.1429	0.66
Meudon	3.34 (3)	1.18	148.6	1.0000	0.76

TABLE 2

MEUDON MODEL PARAMETERS

Parameter	Value
Blackbody temperature	150,000 K
Blackbody radius	10^{10} cm
Inner radius	10^{17} cm
log (H density)	3.4771213
log (He/H)	−1
Log (C/H)	−3.523
log (N/H)	−4
log (O/H)	−3.222
log (Ne/H)	−3.824
log (Mg/H)	−4.523
log (Al/H)	−7
log (Si/H)	−4.523
log (S/H)	−4.824
log (Ar/H)	−9
log (Ca/H)	−7
log (Fe/H)	−7

in the model. The result of the above procedure was $f = 0.76$, which exactly matches the value in column (6) of Table 1. Thus we are confident that our approximation and the results for the nebulae are valid.

3. PHOTOIONIZATION RESULTS

In this section, we wish to further examine the effects of dust on certain observable quantities in PNs. For this purpose, we have again used the Meudon model, whose parameters were discussed in the previous section. We have run several models in which we varied both the dust-to-gas ratio and the hydrogen density, N_H, while keeping all other parameters constant. Although this changes the physical structure of the nebula, it is instructive for giving one a feel for how the nebular quantities vary.

We have examined two quantities: the line ratio He I λλ10830/5876 and the IR luminosity relative to Hβ. Here we take the IR luminosity to be the total luminosity reradiated by grains. The results of the modeling are presented graphically in Figure 1. Figure 1*a* shows the variation of the λλ10830/5876 ratio as a function of the dust-to-gas ratio (again expressed relative to the ISM) for several different values of N_H. In all models, the total hydrogen density, as well as the dust-to-gas ratio, is assumed to be constant throughout the nebula. Figure 2*a* shows the same relation for the ratio $L(\mathrm{IR})/L(\mathrm{H}\beta)$. These results are discussed in the next section.

It is also interesting to examine what effect dust has on the general structure of a PN. We have run the Meudon model with a dust-to-gas ratio equal to that of the ISM and have plotted several quantities as a function of nebular radius. Similar studies have been conducted by Baldwin et al. (1991) and Borkowski & Harrington (1991). In these models, we have assumed a grain composition comparable to the ISM (Martin & Rouleau 1990); i.e., both graphite and silicates are included. We note that the optical properties of the grains were determined from observational fits to the general ISM; therefore the results are not dependent on the precise composition of the grains. Figures 2*a* and 2*b* show the ionization structure of helium and oxygen, respectively. Figure 2*c* shows the grain temperature. In this and the next two figures, graphite and silicates are represented by solid and dotted lines, respectively. Figure 2*d* shows the grain drift velocity and Figure 2*e* the grain potential. Finally the fraction of heating (*solid line*) and cooling (*dotted line*) of the gas due to grains is shown in Figure 2*f*. The results are discussed in the next section.

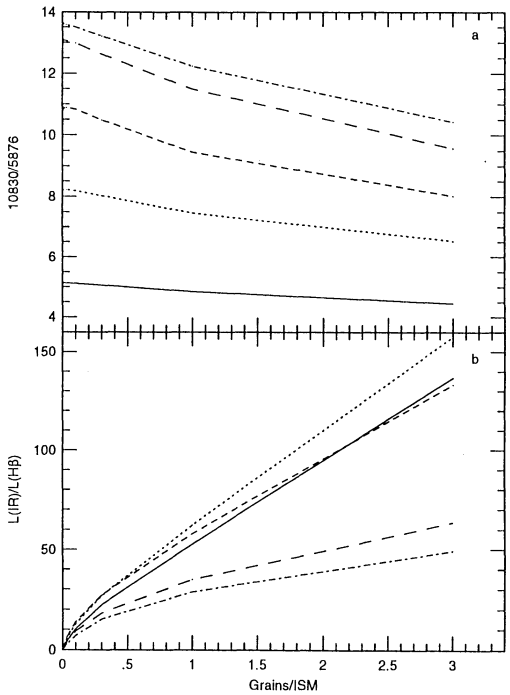

FIG. 1.—(*a*) The λλ10830/5876 intensity ratio is plotted as a function of dust-to-gas ratio for several values of the hydrogen density. Plotted densities are as follows: *solid line*: 10^3; *dotted line*: 3.34×10^3; *short dashed line*: 10^4; *long dashed line*: 5×10^4; *dotted and dashed line*: 10^5. All densities are in cm^{-3}. (*b*) The ratio $L(\mathrm{IR})/L(\mathrm{H}\beta)$ is plotted as a function of dust-to-gas ratio for several values of the hydrogen density. The densities for each line are the same as in (*a*).

4. DISCUSSION AND CONCLUSIONS

We shall now analyze and assess the results of the two previous sections. We begin with the photoionization models of § 3.

The behavior of the ratio λλ10830/5876 as shown in Figure 1*a* is quite straightforward. Since λ10830 is largely produced by collisions, one expects that an increase in density would result in an increase in the λ10830 line intensity. Although λ5876 is also collisionally enhanced, the effect is significantly less. Thus we expect λλ10830/5876 to increase with density as predicted.

Likewise, as discussed previously, because the optical depth in λ10830 can be large in PNs, the line can be significantly destroyed by dust grains. Since λ5876 is unaffected by dust, the λλ10830/5876 ratio should decrease with increasing dust. However, as Figure 1*a* shows, the decrease is very gradual, and the effects of dust only become significant for dust-to-gas ratios comparable to the ISM. We emphasize that the behavior depicted in Figure 1*a* is completely different from the results of § 2, which give the error in the calculated λ10830 intensity for a *given* amount of dust *if* the dust is not included in the line transfer.

In Figure 1*b*, we see that the ratio $L(\mathrm{IR})/L(\mathrm{H}\beta)$ increases with increasing dust content for any density. This is expected since an increase in the amount of dust will clearly increase the net heating of dust grains, and thus their IR emission.

The behavior of $L(\mathrm{IR})/L(\mathrm{H}\beta)$ with density needs some clarification. It appears from Figure 1*b* that for a given dust-to-gas ratio, $L(\mathrm{IR})/(\mathrm{H}\beta)$ increases with increasing density, then decreases with density, with a peak at roughly 1×10^4. This is actually due to a change in the geometry of the model with density. At low densities, the model is spherical, then becomes a thick shell, and finally becomes plane-parallel for large den-

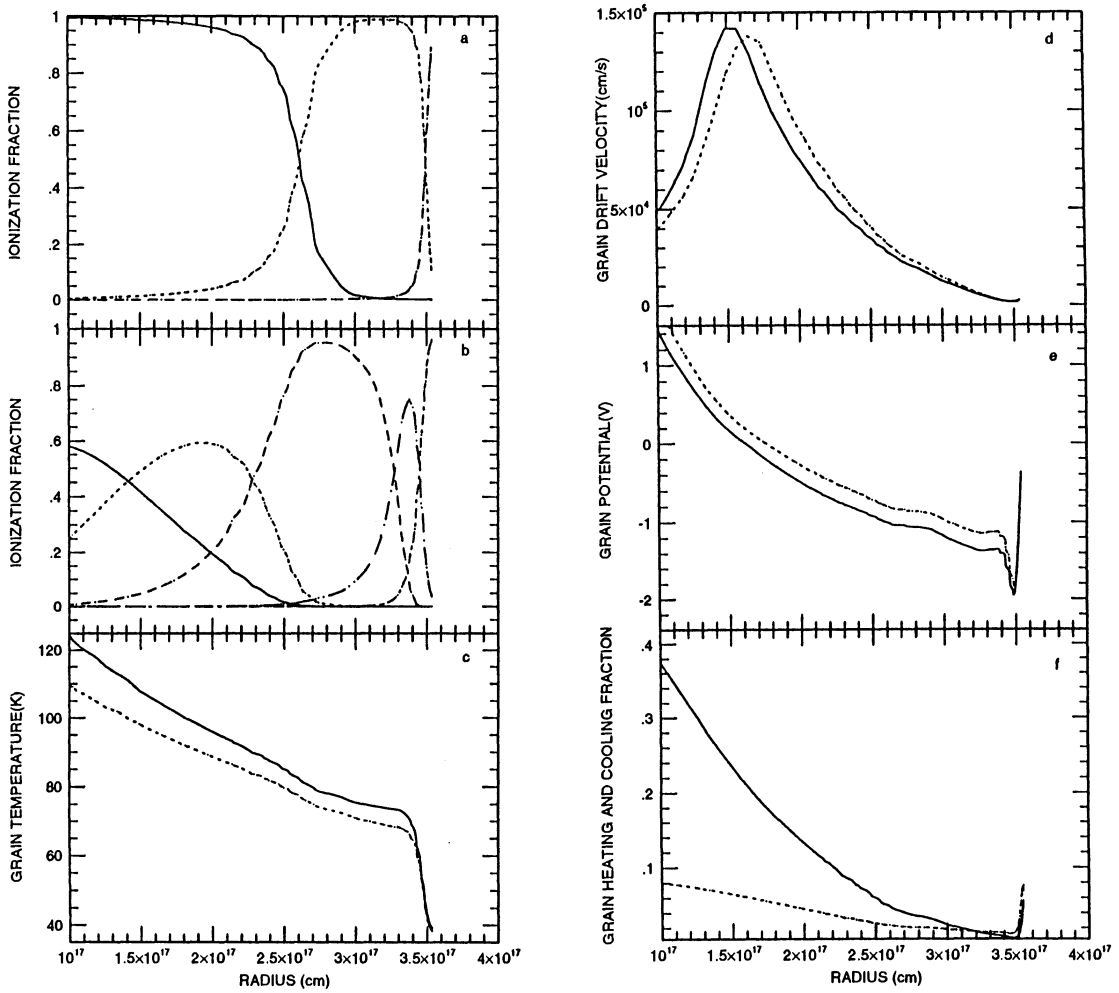

FIG. 2.—(*a*) The He ionization structure, plotted as a function of nebular radius. (*b*) The O ionization structure, plotted as a function of nebular radius. (*c*) Gain temperature as a function of nebular radius. The solid line is for graphite; the dotted line for silicates. (*d*) Grain drift velocity as a function of nebular radius. The solid line is for graphite; the dotted line for silicates. (*e*) Grain potential as a function of nebular radius. The solid line is for graphite; the dotted line for silicates. (*f*) The fraction of nebular heating and cooling due to grains as a function of nebular radius. The solid line shows the heating; the dotted line the cooling. Both grain types are included.

sities. This causes the hydrogen column densities to exhibit a rise and fall with density. If we constrain our model to be plane-parallel for all densities, $L(\mathrm{IR})/L(\mathrm{H}\beta)$ is a monotonically decreasing function of density. This is due to a decrease of column density with electron density, which in turn causes a decrease in the dust optical depth. In effect, the greater the density, the less important dust becomes compared to gas in absorbing radiation.

The grain temperature throughout the model is around 75–125 K, with a pronounced drop occurring for both grain types as the neutral edge of the nebula is encountered. The steady fall in temperature is due to the attenuation of the incident ionizing continuum, which is a primary grain heating source.

The grain drift velocity depicted in Figure 2*d* is the result of the interplay between the radiative acceleration imparted to the dust by the radiation field and the drag forces within the nebula. From this figure, it can be seen that over a typical PN lifetime, the grains will drift about 10^{16} cm relative to the gas, a negligible amount compared to the nebular size. The grain potential results from a combination of ionization and recombination effects. As seen in Figure 2*e*, the potential for both grain types drops steadily until the neutral edge is encountered. This results from the attenuation of the incident continuum, which causes photoinjection of electrons from the grain surface. Far out in the nebula, capture of electrons tends to make the grains negatively charged (cf. Osterbrock 1989).

Grains heat a nebula by providing electrons to the gas via photoionization and cool the nebula by collisions with electrons. As Figure 2*f* shows, the fraction of total heating due to grains (both graphites and silicates) drops with radius, again due to the decrease in photoejection caused by the attenuation of the incident radiation. Grain photoionization can be seen to be a major heating source in the inner ionized region of the nebula. This is because the gas photoelectric opacity is diminished (the gas is highly ionized) so that grains are by far the dominant opacity source. Since the cooling depends largely on the average electron kinematic temperature, one would expect it to show less variation with radius, as is the case here.

Next, we wish to discuss the results of § 2. As Table 1 clearly shows, the effect of including dust in the line transfer of λ10830 is significant for PNs with large optical depths in λ10830. We illustrate the importance of the dust content in Table 3, where we list f for the Meudon model for several values of the dust-to-

TABLE 3

MEUDON MODEL f RESULTS FOR VARIOUS DUST/GAS RATIOS

T_e (1)	τ(10830) (2)	Dust/Gas (3)	f (4)
1.11.....	218.0	0.10	0.95
1.14.....	195.0	0.30	0.89
1.18.....	148.6	1.00	0.76
1.21.....	96.0	3.00	0.65

gas ratio. Columns (1) and (2) list the average electron temperature and mean optical depth in λ10830, respectively. (These were determined from photoionization models.) Column (3) gives the dust-to-gas ratio relative to the ISM, and column (4) gives the values of f. An average electron density of 3.34×10^3 was used throughout. We have included the Meudon result from Table 1 for reference. As is evident from the table, f is a strong function of the dust content. We also note that the electron temperature is a weak function of dust content.

The results of Table 3 are important since the dust content of PNs is not agreed upon and is a topic of some debate. Early attempts to determine dust mass relied on middle-IR observations which missed large, cool grains and therefore greatly underestimated the amount of dust (cf. Balick 1978). Even with careful far-IR observations, the lack of knowledge concerning the size distribution, composition, and emissivity of the grains causes the amount of dust to be underestimated by a factor of ~2 (cf. Natta & Panagia 1976). This suggests that the f values given in Table 1 may in fact be only lower limits.

A recent study which has important implications for the determination of dust-to-gas ratios in PNs is that of Mallik & Peimbert (1988). From an examination of a large number of PNs whose distances were determined independently of any statistical distance scale, they found that the filling factor ε for these objects is much smaller than has been previously assumed. This in turn implies that the ionized gas mass, which is directly proportional to the filling factor, has also been overestimated. Mallik & Peimbert recompute dust-to-gas ratios for several nebulae using their modified values of ε and find an average value of 5.2×10^{-3}, which is roughly three-quarters the value for the general ISM. For the one object in our Table 1 considered by Mallik & Peimbert, IC 418, their dust-to-gas ratio is roughly 2.5 times that which we used. If we recalculate the function f for this new value, we now obtain 0.86, a reduction of 7%. This value is certainly significant. It is imperative that further work along the lines of the Mallik & Peimbert study be conducted to verify their results. If correct, dust will play an even more substantial role in PNs than is currently believed.

Finally, we return to the question of how much of the observed observational to predicted discrepancy in the λ10830 intensity is due to dust. Peimbert & Torres-Peimbert found an observed to predicted λ10830 intensity of ~0.55 for the well-suited PN NGC 7027. To the extent that the Meudon model is an accurate representation of the object, we see from Table 3 that we would require a dust content of greater than 3 times that found in the ISM in order for dust alone to account for the discrepancy. However, since Kingdon & Ferland (1991) found that telluric absorption reduces the λ10830 line intensity by ~22%, we would require only a dust content comparable to the ISM to completely resolve the discrepancy.

In any discussion of the observed intensity of λ10830, it is also important to realize that this line lies in a wavelength regime that is often near the tail of detector sensitivity, both for optical and IR detectors. The observational uncertainties can thus be appreciable, a fact which is usually ignored in regard to this problem. As an example, we note that recent observations of NGC 7027 by Rudy et al. (1992) found a value of λ10830/Hβ equal to 1.66, a value *greater* than that predicted by theory (we derive a value of ~1.30 for this object, ignoring dust). This can be compared with the value 1.05 found by Scrimger (1984), which was used as the basis of the claim that the $2\,^3S$ level is underpopulated. Although Scrimger's observations were made near the maximum of telluric absorption and the Rudy et al. observations were made near the minimum (see Kingdon & Ferland 1991), this discrepancy cannot be explained by this effect alone. As stressed in the last reference, careful observations of λ10830 are essential in order to resolve this problem.

In summary, we have found that dust can significantly decrease the λ10830 line intensity in some PNs, but its role in resolving the λ10830 discrepancy is hampered by serious uncertainties in nebular dust content. It appears, however, that for reasonable underestimates of the dust mass, dust, along with telluric absorption and observational errors, could account for much of the observed intensity reduction.

The authors acknowledge the support of the NSF through grant AST 90-19692, and the useful suggestions of the referee.

REFERENCES

Baldwin, J. A., Ferland, G. J., Martin, P. G., Corbin, M. R., Costa, S. A., Peterson, B. M., & Slettebak, A. 1991, ApJ, 374, 580
Balick, B. 1978, in IAU Symp. 76, Planetary Nebulae, ed. D. R. Flower (Dordrecht: Reidel), 275
Berrington, K. A., Burke, P. G., Freitas, L., & Kingston, A. E. 1985, J. Phys. B, 18, 4135
Berrington, K. A., & Kingston, A. E. 1987, J. Phys. B, 20, 6631
Borkowski, K. J., & Harrington, J. P. 1991, ApJ, 379, 168
Clegg, R. E. S. 1987, MNRAS, 229, 31P
Clegg, R. E. S., & Harrington, J. P. 1989, MNRAS, 239, 869
Draine, B. T., & Lee, H. M. 1984, ApJ, 285, 89
Ferland, G. J. 1986, ApJ, 310, L67
———. 1992, Hazy, OSU Internal Report 92.01
Hummer, D. G. 1968, MNRAS, 138, 73
———. 1981, J. Quant. Spectros. Rad. Transf., 26, 187
Kingdon, J., & Ferland, G. J. 1991, PASP, 103, 752
———. 1993, ApJ, submitted
LeVan, P. D., & Rudy, R. J. 1983, ApJ, 272, 137
Mallik, D. C. V., & Peimbert, M. 1988, Rev. Mexicana Astron. Af., 16, 111
Martin, P. G., & Rouleau, F. 1990, in Extreme Ultraviolet Astronomy, ed. R. F. Malina & S. Boyer (Oxford: Pergamon), 341
Natta, A., & Panagia, N. 1976, A&A, 50, 19
Netzer, H., Elitzur, M., & Ferland, G. J. 1985, ApJ, 299, 752
Osterbrock, D. E. 1964, ARA&A, 2, 95
———. 1989, Astrophysics of Gaseous Nebulae and Active Galactic Nuclei (Mill Valley, CA: Univ. Science Books)
Piembert, M., & Torres-Peimbert, S. 1987, Rev. Mexicana Astron. Af., 15, 117
Péquignot, D. ed. 1986, Workshop on Model Nebulae, (Paris: l'Observatoire de Paris) 363
Péquignot, D., Baluteau, J.-P., & Gruenwald, R. B. 1988, A&A, 191, 278
Persson, S. E. 1970, ApJ, 161, L51
Robbins, R. R. 1970, ApJ, 160, 519
Rudy, R. J., Erwin, R., Rossano, G. S., & Puetter, R. C. 1992, ApJ, 384, 536
Savage, B. D., & Mathis, J. S. 1979, ARA&A, 17, 73
Scrimger, J. N. 1984, ApJ, 280, 170